2011 American Control Conference
on O'Farrell Street, San Francisco, CA, USA
June 29 - July 01, 2011

Multi-Rate Networked Control of Conic (Dissipative) Systems

Nicholas Kottenstette, Heath LeBlanc, Emeka Eyisi, Xenofon Koutsoukos
ISIS/Vanderbilt University

***Abstract*— This paper presents a novel multi-rate digital-control system which preserves stability while providing robustness to time-delay and data loss. In addition, this architecture allows for high-order anti-aliasing filters to be included which do not adversely affect system stability. Therefore, it allows for improved noise-rejection and system performance as compared to traditional digital control systems. It is shown that this framework, based on passivity-based networked control principles, can be used to control not only passive-(dissipative) systems (systems inside the sector $[0, \infty]$) but conic-(dissipative) systems which are inside the sector $[a, b]$ in which $|a| < b$, $0 < b \leq \infty$. We demonstrate the applicability of our result through the *direct position* control of a single-degree of freedom haptic paddle which is inside the sector $[-\tau, \infty]$ in which $0 < \tau < \infty$.**

I. INTRODUCTION

Our team has investigated the use of passivity for the design of Networked Control Systems (NCS) [1] in the presences of time-varying delays [2], [3]. This paper presents an important new step in the design of networked control systems as it applies to control of a conic-(dissipative) plant inside the sector $[a, b]$ in which $|a| < b$, $0 < b \leq \infty$. Passive systems [4] are a special case of conic-(dissipative) systems inside the sector $[0, \infty]$, thus this paper expands the applicability of our framework.

Our approach employs wave variables to transmit information over the network for the feedback control while remaining passive when subject to arbitrary fixed time delays and data dropouts [5], [6]. The primary advantage of using wave variables is that they tolerate most time-varying delays, such as those occurred when using the TCP/IP transmission protocol. In addition, our architecture adopts a multi-rate digital control scheme to account for: i) different time scales at different part of the network; and ii) bandwidth constraints.

This paper provides sufficient conditions for stability of conic systems that are interconnected over wireless networks, and which can tolerate networked delays and data loss. The continuous-time bounded results can be achieved for linear and nonlinear conic systems. The paper also demonstrates how the proposed architecture can be implemented using a new linear passive sampler. Finally, our architecture can be used to isolate wideband and correlated noise without affecting stability through the use of a discrete-time anti-aliasing filter $H_{LP}(z)$ which was synthesized by applying the conic-preserving IPESH-Transform to a high-order Butterworth filter $H_{LP}(s)$.

[0]Contract/grant sponsor (number): NSF (NSF-CCF-0820088)
Contract/grant sponsor (number): NSF (NSF-CNS-1035655)
Contract/grant sponsor (number): Air Force (FA9550-06-1-0312)
Contract/grant sponsor (number): U.S. Army Research Office (ARO W911NF-10-1-0005)
Contract/grant sponsor (number): Lockheed Martin

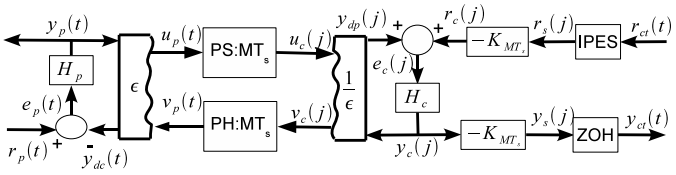

Fig. 1. High Performance, multi-rate digital control network for continuous-time systems.

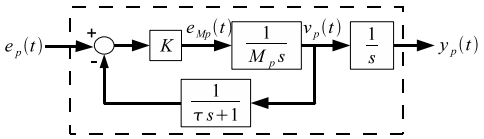

Fig. 2. Plant Dynamics $H_p(s)$

In order to motivate our analysis, Section II recalls the classic point mass model for a single degree of freedom haptic paddle in which we wish to directly control by using position feedback instead of indirectly using velocity feedback. Section III describes our new high-performance digital control system and provides the analysis and stability results. Section IV validates our results by applying our architecture to control the position of a simulated single degree of freedom haptic paddle. Section V provides the conclusions of our paper.

II. MOTIVATION

In [2] we proved that a fixed-rate ($M = 1$) *digital control* framework depicted in Fig. 1 could be used to control the position of a nonlinear robotic systems H_p by i) rendering it strictly output passive (inside the sector $[0, b_p]$, $b_p < \infty$) with velocity feedback and gravity compensation; and ii) applying a digital controller H_c to indirectly control the robot's position by integrating its velocity error $e_c(j)$ with a lag compensator. As a result of being restricted to use indirect velocity feedback, the robotic manipulators position may drift due to imperfect cancellation of gravitational effects, contacting immovable obstacles, and losing data. One way to address this drift problem is to directly control the position of the robot $y_p(t)$; however, it is well known that the relationship between the position of the robot and the controlling torque input $e_{Mp}(t)$ is not passive, a sufficient condition required of the earlier results presented in [2]. Therefore, we will show how to weaken this condition such that the continuous-time plant is only required to be a conic

(dissipative) system inside the sector $[a_p, b_p]$ $|a_p| < b_p \leq \infty$ and derive the corresponding conditions required of the digital controller inside the sector $[a_c, b_c]$.

For simplicity of discussion, we will neglect gravitational effects and consider a *LTI* model of a single degree of freedom haptic paddle with mass M_p which is subject to a low-pass filtered velocity feedback whose time constant is $\tau > 0$ as depicted in Fig. 2. By selecting $K = \frac{M_p}{\tau}$, the resulting transfer function for this system is $H_p(s) = \frac{Y_p(s)}{E_p(s)} = \frac{\tau s+1}{s(\tau^2 s^2+\tau s+1)}$ which is clearly not positive real (or equivalently passive) [7]. However the following system $H(s) = (H_p(s) + \tau)$ is indeed passive as it has the following three required properties [7, Theorem 3] i) all elements of $H(s)$ are analytic in $\mathsf{Re}[s] > 0$, ii) $H(-j\omega) + H(j\omega) \geq 0$ for all $\omega \in \mathbb{R}$ in which $j\omega$ ($\neq j0$) is not a pole of $H(s)$, and iii) for the only simple pure imaginary pole $j\omega_o = j0$ our associated residue matrix $H_o = \lim_{s \to j\omega_o}(s - j\omega_o)H(s) = 1$ is clearly nonnegative definite Hermitian ($H_o = H_o^* \geq 0$). One important property of passive systems such as $H(s)$ is that they are Lyapunov stable as a result $H_p(s) = H(s) - \tau$ is obviously Lyapunov stable as well. In addition both systems are *interior conic-dissipative systems* in which $H(s)$ is *inside the sector* $[0, \infty]$ (as are all linear and nonlinear passive-dissipative systems) and $H_p(s)$ is inside the sector $[-\tau, \infty]$ (as are many Lyapunov stable dissipative systems which have the same number of inputs and outputs). Additional details with respect to interior conic-dissipative systems, their properties and the system architecture are presented in Section III.

III. High Performance Digital Control Networks

Fig. 1 depicts a multi-rate digital control network which interfaces a conic digital controller $H_c : e_c \to y_c$ to a continuous-time conic plant $H_p : e_p \to y_p$ [8]–[10]. The digital control network is a hybrid network consisting of both continuous-time wave variables $(u_p(t), v_p(t)))$ and discrete-time wave variables $(u_c(j), v_c(j))$ in which $j = \lfloor \frac{t}{MT_s} \rfloor$ [5], [6], [11]. The relationships between the continuous-time and discrete-time wave variables is determined by the multi-rate passive sampler (denoted $\mathsf{PS} : MT_s$) and multi-rate passive hold (denoted $\mathsf{PH} : MT_s$). These two elements are a combination of the passive sampler and passive hold blocks (which have been instrumental in showing how to interconnect digital controllers to continuous-time systems in order to achieve L_2^m-stability [2], [11]; see [12]–[15] for interconnecting continuous-time plants to continuous-time controllers over digital networks) and a discrete-time passive upsampler and passive downsampler [3]. At the interface to the digital controller is an inner product equivalent sample (IPES) and zero-order (ZOH) hold block $y_{ct}(t) = y_s(j),\ t \in [jMT_s, (j+1)MT_s)$ [11] which are used *for analysis* in order to relate continuous-time control inputs $r_{ct}(t)$ and continuous-time control outputs $y_{ct}(t)$ to the continuous-time plant inputs $r_p(t)$ and outputs $y_p(t)$.

The architecture has the following advantages over traditional digital control systems: 1) L_2^m-stability can be guaranteed for all (non)linear (dissipative)-conic plants H_p inside the sector $[a_p, b_p]$ in which $|a_p| < b_p$, $0 \leq b_p \leq \infty$; 2) the $\mathsf{PS} : MT_s$ can be implemented as a high order anti-aliasing filter in order to more effectively remove wideband, and correlated noise introduced into the signal $y_p(t)$ without adversely affecting stability.

By choosing, to use wave variables, a negative output feedback loop is introduced for both the plant and controller in which we provide the analysis to determine its effects in Section III-A. Section III-B presents the multi-rate passive sampler and multi-rate passive hold which consists of a *simplified linear* passive sampler and our main stability results. Section III-C provides the necessary results to construct conic digital filters (which are inside the sector $[a_f, b_f]$ from conic continuous-time filters which are inside the sector $[a_f, b_f]$.

A. Control of Conic-Dissipative Systems

In order to leverage the pioneering work of [8], [9] in regards to the control of conic systems and connect it to dissipative systems theory [16], we shall consider the following class of causal nonlinear finite-dimensional continuous-time (discrete-time) systems $H : u \to y$ which are affine in control:

$$\begin{aligned} \dot{x}(t) &= f(x(t)) + G(x(t))u(t),\ x(0) = x_0 = 0,\ t \geq 0 \\ y(t) &= h(x(t)) + J(x(t))u(t) \end{aligned} \quad (1)$$

for the continuous-time case in which the functions indicated in (1) are sufficiently smooth to make the system well defined [17], and

$$\begin{aligned} x(j+1) &= f(x(j)) + G(x(j))u(j),\ x(0) = x_0 = 0 \\ y(j) &= h(x(j)) + J(x(j))u(j) \end{aligned} \quad (2)$$

for the discrete time case ($j = \{0, 1, \dots\}$) in which $x \in \mathbb{R}^n$, $u, y \in \mathbb{R}^m$ in which n and m are positive integers. In addition it is assumed that there exists a finite square-integrable (summable) function $u(\cdot)$ such that all $x \in \mathbb{R}^n$ are reachable from the zero-state x_0. Finally it is assumed that x_0 is the only equilibrium point such that $f(x_0) = 0$ and $f(x) \neq 0$ when $x \neq x_0$. Finally, we shall consider the following interior conic-dissipative supply function $s(u, y)$ as it relates to conic-dissipative systems which are inside the sector $[a, b]$ ($a < b$) [18]–[20]:

$$s(u,y) = \begin{cases} -y^{\mathsf{T}}y + (a+b)y^{\mathsf{T}}u - abu^{\mathsf{T}}u,\ |a|, |b| < \infty \\ y^{\mathsf{T}}u - au^{\mathsf{T}}u,\ |a| < \infty,\ b = \infty. \end{cases} \quad (3)$$

Definition 1: The continuous-time system $H : u \to y$, $x_0 = x(0) = 0$ whose dynamics are determined by (1) is a continuous conic-dissipative system inside the sector $[a, b]$ with respect to the supply (3) if:

$$\int_0^T s(u,y)dt \geq 0,\ T \in \mathbb{R}^+. \quad (4)$$

Analogously the discrete-time system $H : u \to y$, $x_0 = x(0) = 0$ whose dynamics are determined by (2) is a discrete

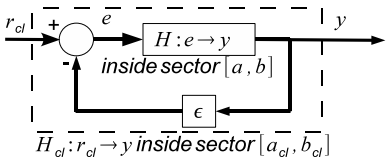

Fig. 3. Nominal closed-loop system H_{cl} resulting from ϵ and H.

conic-dissipative system inside the sector $[a, b]$ with respect to the supply (3) if:

$$\sum_{j=0}^{N-1} s(u, y) \geq 0, \ \forall N \ \in \ \{1, 2, \dots\}. \tag{5}$$

NB. the smoothness condition required by [17] appears to limit the discussion to systems which have finite state space descriptions and the resulting control system we will examine will be subject to time delays which result in an infinite state space. Therefore, if functions indicated in (1) are *not* sufficiently smooth but (4) is satisfied then the system $H : u \to y$ is a *continuous conic system* inside the sector $[a, b]$. Finally the following notation will be used in order to represent time integrals, sums and norms:

$$\langle y, u \rangle_T = \int_0^T y^{\mathsf{T}}(t) u(t) dt; \quad \|(y)_T\|_2^2 = \langle y, y \rangle_T$$
$$\langle y, u \rangle_N = \sum_{j=0}^{N-1} y^{\mathsf{T}}(j) u(j); \quad \|(y)_N\|_2^2 = \langle y, y \rangle_N$$
$$\|y(t)\|_2^2 = \lim_{T \to \infty} \|(y)_T\|_2^2; \quad \|y(j)\|_2^2 = \lim_{N \to \infty} \|(y)_N\|_2^2.$$

If it is clear that y is either a continuous or discrete-time function then the two-norm of y will be denoted simply $\|y\|_2$.

From [17], [20] in regards to Lyapunov stability and from [8]–[10] in regards to L_2^m (l_2^m) stability conic-dissipative systems have the following important properties:

Property 1: There exists a storage function $V(x) \geq 0$ $\forall x \neq 0, V(0) = 0$ such that $\dot{V}(x) \leq s(u, y)$ for a continuous conic-dissipative system and $V(x(j+1)) - V(x(j)) \leq s(u(j), y(j))$ for a discrete-time conic-dissipative system. Therefore if $H : u \to y$ is inside the sector $[a, b]$:

i) and zero-state detectable [1](implies $V(x) > 0$ $\forall x \neq 0$) and $|a| < \infty$, $b = \infty$ it is Lyapunov stable.
ii) and zero-state detectable and $|a|, |b| < \infty$ it is asymptotically stable.
iii) and $|a|, |b| < \infty$ then it is inside the sector $[-\gamma, \gamma]$ in which $\gamma = \max\{|a|, |b|\}$. Therefore, it is $L_2^m(l_2^m)$-stable in which:
$$\|y\|_2 \leq \gamma \|u\|_2. \tag{6}$$
iv) and $k \geq 0$ then kH is inside the sector $[ka, kb]$; $-kH$ is inside the sector $[-kb, -ka]$.
v) (Sum Rule) if in addition $H_1 : u_1 \to y_1$ is inside the sector $[a_1, b_1]$ then $(H + H_1) : u \to (y + y_1)$ is inside the sector $[a + a_1, b + b_1]$.

We are particularly interested in determining the resulting gain $g(H_{\mathsf{cl}})$ ($\|(y)_T\|_2 \leq g(H_{\mathsf{cl}}) \|(r_{\mathsf{cl}})_T\|_2$) when closing the loop of a conic system H which is inside the sector $[a, b]$ as depicted in Fig. 3.

Theorem 1: Let the conic system $H : e \to y$ depicted in Fig. 3 be inside the sector $[a, b]$, $\epsilon > 0$. The input e is related to the reference r_{cl} and output y by the following feedback equation: $e(t) = r_{\mathsf{cl}}(t) - \epsilon y(t), \ \forall t \geq 0$. The resulting closed-loop system is denoted $H_{\mathsf{cl}} : r_{\mathsf{cl}} \to y$. For the case when:

I. $0 \leq a < b \leq \infty$, H_{cl} is inside the sector $[\frac{a}{1+\epsilon a}, \frac{b}{1+\epsilon b}]$ in which $g(H_{\mathsf{cl}}) = \frac{b}{1+\epsilon b}$.
II. $a < 0$, $-a < b \leq \infty$, $0 \leq \epsilon < -\frac{1}{2}\left(\frac{1}{a} + \frac{1}{b}\right)$ then H_{cl} is inside the sector $[\frac{a}{1+\epsilon a}, \frac{b}{1+\epsilon b}]$ in which $g(H_{\mathsf{cl}}) = \frac{b}{1+\epsilon b}$.

See proof in [21].

1) Wave Variable Networks: In order to analyze the closed-loop effects on H_p and H_c we recall our use of wave variables. As discussed in [11], scattering [22] – or their reformulation known as the wave variable networks – allow *controller* and *plant* variables $(y_c(j), y_p(t))$, to be transmitted over a network while remaining *passive* when subject to arbitrary fixed time delays and data dropouts [5]. Denote $I \in \mathbb{R}^{m \times m}$ as the identity matrix. When implementing the wave variable transformation the continuous time plant "outputs" $(u_p(t), y_{\mathsf{dc}}(t))$ are related to the corresponding "inputs" $(v_p(t), y_p(t))$ as follows (Fig. 1):

$$\begin{bmatrix} u_p(t) \\ y_{\mathsf{dc}}(t) \end{bmatrix} = \begin{bmatrix} -I & \sqrt{2\epsilon} I \\ -\sqrt{2\epsilon} I & \epsilon I \end{bmatrix} \begin{bmatrix} v_p(t) \\ y_p(t) \end{bmatrix} \tag{7}$$

Next, the discrete time controller "outputs" $(v_c(j), y_{\mathsf{dp}}(j))$ are related to the corresponding "inputs" $(u_c(j), y_c(j))$ as follows (Fig. 1):

$$\begin{bmatrix} v_c(j) \\ y_{\mathsf{dp}}(j) \end{bmatrix} = \begin{bmatrix} I & -\sqrt{\frac{2}{\epsilon}} I \\ \sqrt{\frac{2}{\epsilon}} I & -\frac{1}{\epsilon} I \end{bmatrix} \begin{bmatrix} u_c(j) \\ y_c(j) \end{bmatrix} \tag{8}$$

It has been shown that the digital control network for $M = 1$ depicted in Fig. 1 results in a L_2^m-stable system *if the discrete-time controller H_c is strictly output passive (inside the sector $[0, b_c]$) and the continuous-time plant H_p is strictly output passive (inside the sector $[0, b_p]$)* [2], [11]. In order to study the case when H_p is not passive we need to: i) explicitly consider the network structure which results from using wave variables; and ii) use Assumption 1.

Assumption 1: The plant depicted in Fig. 1 H_p is inside the sector $[a_p, b_p]$; in addition the controller H_c is inside the sector $[a_c, b_c]$ ($a_c \geq 0$); the scattering gain ϵ satisfies the following bounds: i) $0 < \epsilon < \infty$, if $a_p \geq 0$; or ii) $0 < \epsilon < -\frac{1}{2}\left(\frac{1}{a_p} + \frac{1}{b_p}\right)$, if $a_p < 0$.

Assumption 1, Lemma 4 and Lemma 5 (see Appendix) allow us to state Theorem 2.

Theorem 2: The plant-controller network depicted in Fig. 1 can be transformed to the final form depicted in Fig. 4 if Assumption 1 is satisfied. The transformed plant subsystem $\sqrt{2\epsilon} H_{\mathsf{pe}} : \hat{e}_{\mathsf{clp}} \to y_{\mathsf{pe}}$ is denoted with the shorthand notation $\sqrt{2\epsilon} H_{\mathsf{pe}}$ in which: i) $\hat{e}_{\mathsf{clp}}(t) = \frac{1}{\sqrt{2\epsilon}} r_p(t) + v_p(t)$; and ii) $y_{\mathsf{pe}}(t) = \sqrt{2\epsilon} y_p(t) - \hat{e}_{\mathsf{clp}}(t)$ hold. In addition the transformed control subsystem $\sqrt{\frac{2}{\epsilon}} H_{\mathsf{ce}} : \hat{e}_{\mathsf{clc}} \to y_{\mathsf{ce}}$ is denoted

[1]if $u(t) = y(t) = h(x(t)) = 0$ for all $t \geq t_0$ and as $t \to \infty$ $x(t) = 0$

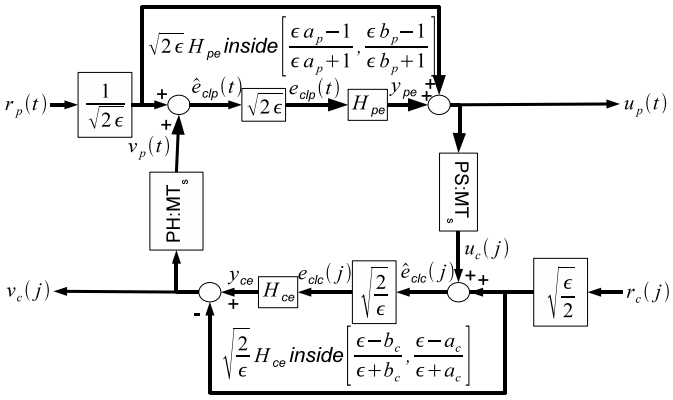

Fig. 4. Final Plant-Controller wave network realization.

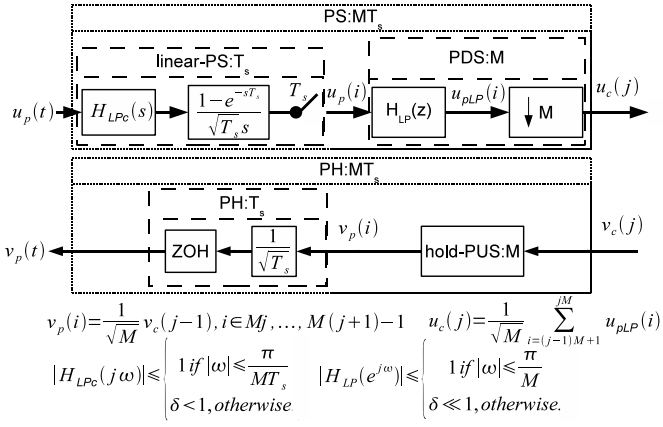

Fig. 5. Multi-rate passive sampler, passive hold.

with the shorthand notation $\sqrt{\frac{2}{\epsilon}}H_{\mathsf{ce}}$ in which: i) $\hat{e}_{\mathsf{clc}}(j) = \sqrt{\frac{\epsilon}{2}}r_c(j)+u_c(j)$; and ii) $y_{\mathsf{ce}}(j) = -\sqrt{\frac{2}{\epsilon}}y_c(j)+\hat{e}_{\mathsf{clc}}(j)$ hold. Each is a conic-dissipative system such that

$$\sqrt{2\epsilon}H_{\mathsf{pe}} \text{ is inside the sector } \left[\frac{\epsilon a_p-1}{\epsilon a_p+1},\frac{\epsilon b_p-1}{\epsilon b_p+1}\right] \text{ and}$$
$$\sqrt{\frac{2}{\epsilon}}H_{\mathsf{ce}} \text{ is inside the sector } \left[\frac{\epsilon-b_c}{\epsilon+b_c},\frac{\epsilon-a_c}{\epsilon+a_c}\right].$$

B. Multi-Rate Passive Sampler(Hold)

Fig. 5 depicts our proposed multi-rate passive sampler (PS:MT_s), and passive hold (PH:MT_s) subsystem. The multi-rate passive sampler (PS:MT_s) consists of a cascade of a linear passive sampler (linear-PS:T_s) and a passive down-sampler (PDS:M). The multi-rate passive hold (PH:MT_s) subsystem consists of a cascade of a hold-passive upsampler (hold-PUS:M) and passive hold (PH:T_s). For simplicity of discussion the figure is for the single-input, single-output (SISO) case but we note all elements depicted can be diagonalized to handle m-dimensional waves. The standard anti-aliasing downsampler $(H_{LP}(z),\downarrow M)$ system depicted in Fig. 5 has been shown to be a PDS, in addition the hold-PUS depicted is a PUS [3, Definition 4]. A valid PDS:M and PUS:M satisfy the following inequalities:

$$\|(u_c(j))_N\|_2^2 \leq \|(u_p(i))_{MN}\|_2^2 \quad (9)$$
$$\|(v_p(i))_{MN}\|_2^2 \leq \|(v_c(j))_N\|_2^2 \quad (10)$$

which hold $\forall N \geq 0$ [2]. The scaled ZOH block in which $v_p(t) = \frac{1}{T_s}v_p(i),\ t\in[iT_s,(i+1)T_s)$ has been shown to be a valid passive hold system PH:T_s in which

$$\|(v_p(t))_{MNT_s}\|_2^2 \leq \|(v_p(i))_{MN}\|_2^2 \quad (11)$$

[2]. A valid passive sampler will satisfy the following inequality

$$\|(u_p(i))_{MN}\|_2^2 \leq \|(u_p(t))_{MNT_s}\|_2^2, \quad (12)$$

unlike the nonlinear averaging passive sampler [11, Definition 6] implementation which was shown to be a valid PS we choose to implement a linear version which is a filtered and appropriately scaled version of the *passive interpolative downsampler* [15] in order to satisfy (12).

Definition 2: The linear passive sampler (Fig. 5) with input $u_p(t)$ and output $u_p(i)$ is implemented as follows:

1. $u_p(t)$ passes through an analog low-pass anti-aliasing filter denoted $H_{\mathsf{LPc}}(s)$ whose magnitude $|H_{\mathsf{LPc}}(j\omega)| \leq 1$ with passband $\omega_p = \frac{\pi}{MT_s}$ and stopband $\omega_s = \frac{\pi}{T_s}$ [23].
2. the output of $H_{\mathsf{LPc}}(s)$ we denote as $u_{pLPc}(t)$ in which

$$u_p(i) = \frac{1}{\sqrt{T_s}}\int_0^{iT_s}(u_{pLPc}(t)-u_{pLPc}(t-T_s))dt \quad (13)$$

Lemma 1: The linear passive sampler (Definition 2) satisfies (12).

See proof in [21]. Finally, from (9) and (12) it is obvious that the following inequality holds for the multi-rate passive sampler PS:MT_s

$$\|(u_c(j))_N\|_2^2 \leq \|(u_p(t))_{MNT_s}\|_2^2 \quad (14)$$

and from (11) and (10) the following holds for the multi-rate passive hold PH:MT_s

$$\|(v_p(t))_{MNT_s}\|_2^2 \leq \|(v_c(j))_N\|_2^2 \quad (15)$$

With these two inequalities established, and Theorem 2 we can now prove the following Lemma.

Lemma 2: Denote the L_2^m-gain of the plant subsystem $\sqrt{2\epsilon}H_{\mathsf{pe}} : \hat{e}_{\mathsf{clp}} \rightarrow y_{\mathsf{pe}}$ as γ_{pe} in which $\|(y_{\mathsf{pe}})_{MNT_s}\|_2 \leq \gamma_{\mathsf{pe}}\|(\hat{e}_{\mathsf{clp}})_{MNT_s}\|_2$. In addition, denote the l_2^m-gain of the controller subsystem $\sqrt{\frac{2}{\epsilon}}H_{\mathsf{ce}} : \hat{e}_{\mathsf{clc}} \rightarrow y_{\mathsf{ce}}$ as γ_{ce} in which $\|(y_{\mathsf{ce}})_N\|_2 \leq \gamma_{\mathsf{ce}}\|(\hat{e}_{\mathsf{clc}})_N\|_2$. In addition we shall use the following shorthand notation in which $\hat{E}_{\mathsf{clp}} = \|(\hat{e}_{\mathsf{clp}})_{MNT_s}\|_2$, $\hat{E}_{\mathsf{clc}} = \|(\hat{e}_{\mathsf{clc}})_N\|_2$, $R_p = \|(r_p)_{MNT_s}\|_2$, and $R_c = \|(r_c)_N\|_2$. If $\gamma_{\mathsf{pe}}\gamma_{\mathsf{ce}} < 1$ then $\hat{E}_{\mathsf{clc}} \leq \frac{\gamma_{\mathsf{pe}}+1}{1-\gamma_{\mathsf{pe}}\gamma_{\mathsf{ce}}}\left(\sqrt{\frac{\epsilon}{2}}R_c + \frac{1}{\sqrt{2\epsilon}}R_p\right)$ and $\hat{E}_{\mathsf{clp}} \leq \frac{\gamma_{\mathsf{ce}}+1}{1-\gamma_{\mathsf{pe}}\gamma_{\mathsf{ce}}}\left(\sqrt{\frac{\epsilon}{2}}R_c + \frac{1}{\sqrt{2\epsilon}}R_p\right)$.

See proof in [21]. Next we note the following observation that $\gamma_{\mathsf{pe}} = g(\sqrt{2\epsilon}H_{\mathsf{pe}}) = g(-\sqrt{2\epsilon}H_{\mathsf{pe}})$ and $\gamma_{\mathsf{ce}} =$

[2]N.B. our downsampling operation is a sampled weighted average $(u_c(j) = \frac{1}{\sqrt{M}}\sum_{i=(j-1)M+1}^{jM}u_{pLP}(i))$ which results in the same inequality given by (9) if $u_c(j) = u_{pLP}(Mj)$.

$g(\sqrt{\frac{2}{\epsilon}}H_{\mathsf{ce}}) = g(-\sqrt{\frac{2}{\epsilon}}H_{\mathsf{ce}})$ therefore using Theorem 1, Theorem 2 the following Corollary follows.

Corollary 1:

$$\gamma_{\mathsf{pe}} = g(\sqrt{2\epsilon}H_{\mathsf{pe}}) = \max\left\{\left|\frac{\epsilon a_p - 1}{\epsilon a_p + 1}\right|, \left|\frac{\epsilon b_p - 1}{\epsilon b_p + 1}\right|\right\} \quad (16)$$

$$\gamma_{\mathsf{ce}} = g(\sqrt{\frac{2}{\epsilon}}H_{\mathsf{ce}}) = \max\left\{\left|\frac{\epsilon - b_c}{\epsilon + b_c}\right|, \left|\frac{\epsilon - a_c}{\epsilon + a_c}\right|\right\} \quad (17)$$

Therefore:

1. when the plant is passive ($a_p = 0$, $b_p = \infty$) then $\gamma_{\mathsf{pe}} = 1$ which implies $\gamma_{\mathsf{pe}}\gamma_{\mathsf{ce}} < 1$ if the controller is strictly input-output passive $0 < a_c \leq b_c < \infty$ (and vice versa).
2. when the plant is inside the sector $[a_p, \infty]$ in which $a_p < 0$ then $\gamma_{\mathsf{pe}}\gamma_{\mathsf{ce}} < 1$ if the controller is inside the sector $[a_c, b_c]$ in which $-\epsilon^2 a_p < a_c, b_c < \frac{-1}{a_p}$.

As was shown in [11] the IPESH blocks can be used to aid with analysis such that

$$\|(y_c)_N\|_2 = \frac{1}{\sqrt{MT_s}K_{MT_s}}\|(y_{ct})_{MNT_s}\|_2 \quad (18)$$

holds. In addition, the following inequality result from applying the *Schwarz inequality* as demonstrated in [24, proof of Theorem 1-III].

$$\|(r_c)_N\|_2 \leq \sqrt{MT_s}K_{MT_s}\|(r_{ct})_{MNT_s}\|_2 \quad (19)$$

Theorem 3: When $\gamma_{\mathsf{pe}}\gamma_{\mathsf{ce}} < 1$ the digital control network depicted in Fig. 1 is L_2^m-stable in which there exists a $0 < \gamma < \infty$ such that $\|y(t)\|_2 \leq \gamma\|u(t)\|_2$ in which $y^{\mathsf{T}}(t) = [y_p^{\mathsf{T}}(t), y_{ct}^{\mathsf{T}}(t)]$ and $u^{\mathsf{T}}(t) = [r_p^{\mathsf{T}}(t), r_{ct}^{\mathsf{T}}(t)]$.

Proof: (Sketch) From Corollary 4 in the Appendix we have that $H_{\mathsf{clc}} : e_{\mathsf{clc}} \to y_c$ has finite gain $g(H_{\mathsf{clc}}) = \frac{\epsilon b_c}{\epsilon + b_c}$ and $\sqrt{\frac{2}{\epsilon}}\hat{E}_{\mathsf{clc}} = \|(e_{\mathsf{clc}})_N\|_2$, therefore $\|(y_c)_N\|_2 \leq \frac{\epsilon b_c}{\epsilon + b_c}\sqrt{\frac{2}{\epsilon}}\hat{E}_{\mathsf{clc}}$ substituting (18) for the left-hand-side results in $\frac{1}{\sqrt{MT_s}K_{MT_s}}\|(y_{ct})_{MNT_s}\|_2 \leq \frac{\epsilon b_c}{\epsilon + b_c}\sqrt{\frac{2}{\epsilon}}\hat{E}_{\mathsf{clc}}$. Similarly $\|(y_p)_{MNT_s}\|_2 \leq \frac{b_p}{1+\epsilon b_p}\sqrt{2\epsilon}\hat{E}_{\mathsf{clp}}$ holds since from Corollary 3 in the Appendix we know that the closed-loop plant $H_{\mathsf{clp}} : e_{\mathsf{clp}} \to y_{\mathsf{clp}}$ has finite gain $g(H_{\mathsf{clp}}) = \frac{b_p}{1+\epsilon b_p}$ and that $\sqrt{2\epsilon}\hat{E}_{\mathsf{clp}} = \|(e_{\mathsf{clp}})_{MNT_s}\|_2$. Finally, we observe that (19) along with the other continuous-time norm inequalities can be substituted into the final two inequalities of Lemma 2 such that both inequalities involve only continuous-time norms in which the outputs $y_p(t)$ and $y_{ct}(t)$ are bounded by the inputs $r_p(t)$ and $r_{ct}(t)$. Therefore, when $\gamma_{\mathsf{pe}}\gamma_{\mathsf{ce}} < 1$ the digital control network depicted in Fig. 1 is L_2^m-stable. ■

C. Conic Digital Filters

The section shows how an engineer can synthesize a discrete-time controller/filter from a continuous-time reference model. In particular, we show how a continuous-time conic system can be transformed into a discrete-time conic system using the *inner product equivalent sample and hold* (IPESH). Additionally, we present a corollary for transforming a continuous-time conic single-input, single-output (SISO) linear time-invariant (*LTI*) system into a discrete-time conic SISO *LTI* system using the IPESH-Transform.

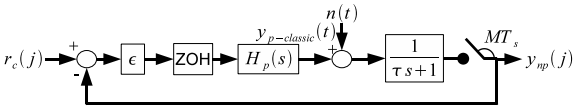

Fig. 6. The classical digital control design for position tracking

We begin by recalling the definition for the IPESH which is based on the earlier work of [25], [26].

Definition 3: [27, Definition 4] Let a continuous one-port plant be denoted by the input-output mapping $H_{ct} : L_{2_e}^m \to L_{2_e}^m$. Denote continuous time as t, the discrete time index as i, the sample and hold time as T_s, the continuous input as $u(t) \in L_{2_e}^m$, the continuous output as $y(t) \in L_{2_e}^m$, the transformed discrete input as $u(i) \in l_{2_e}^m$, and the transformed discrete output as $y(i) \in l_{2_e}^m$. The *inner product equivalent sample and hold* (IPESH) is implemented as follows: I. $x(t) = \int_0^t y(\tau)d\tau$; II. $y(i) = x((i+1)T_s) - x(iT_s)$; III. $u(t) = u(i), \forall t \in [iT_s, (i+1)T_s)$. As a result $\langle y(i), u(i)\rangle_N = \langle y(t), u(t)\rangle_{NT_s}$ holds $\forall N \geq 1$.

Lemma 3: If H_{ct} is inside the sector $[a, b]$ and $|a| < b$ then H_d resulting from the IPESH is inside the sector $[aT_s, bT_s]$.

The IPESH similar to the bilinear transform can be used to synthesize stable digital controllers from continuous-time models. Therefore, we recall the IPESH-Transform definition as it applies to SISO *LTI* systems.

Definition 4: [3, Definition 5] Let $H_p(s)$ and $H_p(z)$ denote the respective continuous and discrete time transfer functions which describe a plant. Furthermore, let T_s denote the respective sample and hold time. Finally, denote $\mathcal{Z}\{F(s)\}$ as the z-transform of the sampled time series whose Laplace transform is the expression of $F(s)$, given on the same line in [28, Table 8.1 p.600]. $H_p(z)$ is generated using the following IPESH-Transform $H_p(z) = \frac{(z-1)^2}{T_s z}\mathcal{Z}\left\{\frac{H_p(s)}{s^2}\right\}$.

N.B. the term $\frac{z-1}{z}\mathcal{Z}\left\{\frac{H_p(s)}{s^2}\right\}$ represents the exact discrete equivalent for the *LTI* system $\frac{H_p(s)}{s}$ preceded by a ZOH [28, p. 622] as noted in a detailed proof of [3, Lemma 5] which shows that the IPESH-Transform is a scaled version ($k = \frac{1}{T_s}$) of the IPESH (Definition 3). The scaling property (Property 1-iv) and Lemma 3 lead directly to Corollary 2.

Corollary 2: If a SISO *LTI* system $H(s)$ is inside the sector $[a, b]$ then $H_p(z)$ resulting from applying the IPESH-Transform to $H_p(s)$ is inside the sector $[a, b]$.

IV. CONTROLLER VALIDATION & SIMULATION

Next, we validate our results through the control of an idealized single degree of freedom haptic paddle as described in Section II and depicted in Fig. 2. This nominal plant system $H_p(s)$ will be controlled using our digital control network depicted in Fig. 1 in which we shall use a proportional controller $y_c(j) = k_c e_c(j)$ in which the gain k_c is chosen to satisfy the conditions in Corollary 1 such that $-\epsilon^2 a_p = \epsilon^2\tau < k_c < \frac{1}{\tau} = -\frac{1}{a_p}$. In addition $K_{MT_s} = \sqrt{MT_s}$ is chosen so that $r_s(j) = y_p(t)$ at steady-state. Fig. 6 depicts

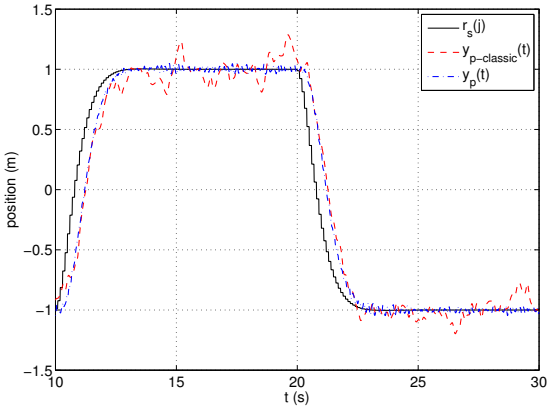

Fig. 7. Baseline tracking response with minimal delay $n(t) \neq 0$.

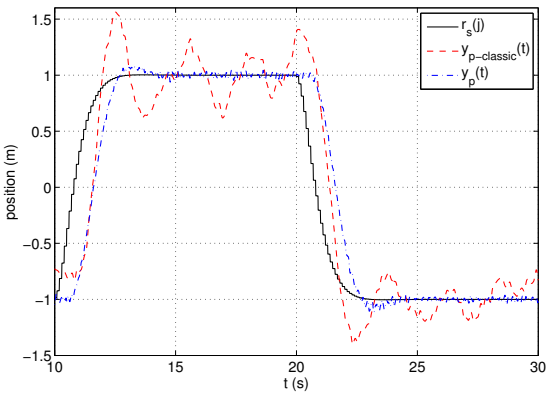

Fig. 8. Position response with 0.5 second delay.

a classic digital position feedback control scheme in which $r_c(j) = y_{p-\text{classic}}(jMT_s)$ at steady-state when $n(t) = 0$.

In order to compare the effects of band-limited noise $n(t)$, the low-pass filtered and noise-corrupted feedback signal $y_{np}(j)$ is periodically sampled every MT_s seconds for the classical scheme whereas the signal y_p depicted in Fig. 1 is corrupted similarly such that $y_p(t) = (H_p e_p(t) + n(t))$. For our high-performance system we filter the noise corrupted signal using the multi-rate passive sampler subsystem (Fig. 5) described in Section III-B in which $H_{\text{LPc}}(s) = \frac{1}{\tau s+1}$. In addition a second stage digital anti-aliasing filter $H_{LP}(z)$ was synthesized by applying the IPESH-Transform to a sixth order low-pass Butterworth filter model $H_{LP}(s)$ with passband $\omega_p = \frac{\pi}{MT_s}$ [23, Section 9.7.5].

The simulation parameters are as follows: $\epsilon = 2$, $M_p = 2$ kg, $T_s = .01$ seconds, $M = 10$, $\tau = \frac{MT_s}{\pi}$, $\frac{.4}{\pi} < k_c = 3 < 10\pi$ and $K_{MT_s} = \sqrt{MT_s}$. Fig. 7 indicates that our high-performance position $y_p(t)$ response tracks the desired reference $r_s(j)$ closer than the classic digital control system response $y_{p-\text{classic}}(t)$ when subject to band-limited noise within the frequency band $[\frac{\pi}{MT_s}, \frac{\pi}{T_s}]$. Finally, Fig. 8 indicates that our proposed system is significantly less sensitive to the introduction of a 0.5 second delay between the controller and the plant.

V. CONCLUSIONS

We have provided a set of sufficient conditions to guarantee delay independent stability for non-passive systems H_p inside the sector $[a_p, b_p]$ $-\infty < a_p < b_p$ for our networked control architecture depicted in Fig. 1. In particular, Theorem 1 and Assumption 1 allow us to derive Theorem 2 which describe the internal network structure depicted in Fig. 4. Lemma 1 shows that a *linear* passive sampler depicted in Fig. 5 satisfied the key inequality (12). As a result linear anti-aliasing filters can be introduced which *do not* adversely affect stability or performance. Lemma 2 and Corollary 1 provide the sufficient sector conditions for the controller and plant to achieve the small gain conditions required of Theorem 3 in order to guarantee L_2^m-stability. Corollary 2 shows that the IPESH-Transform can be applied to an analog controller to synthesize a digital controller such that both controllers are inside the sector $[a, b]$. Simulation results of our proposed architecture applied to *direct position* control of a haptic paddle indicate good performance with low sensitivity to band-limited noise and networked delay.

REFERENCES

[1] P. J. Antsaklis and J. Baillieul, Eds., *Special Issue: Technology of Networked Control Systems*. Proceedings of the IEEE, 2007, vol. 95 no. 1.

[2] N. Kottenstette, X. Koutsoukos, J. Hall, J. Sztipanovits, and P. Antsaklis, "Passivity-Based Design of Wireless Networked Control Systems for Robustness to Time-Varying Delays," *Real-Time Systems Symposium, 2008*, pp. 15–24, 2008.

[3] N. Kottenstette, J. F. Hall, X. Koutsoukos, P. Antsaklis, and J. Sztipanovits, "Digital control of multiple discrete passive plants over networks," *International Journal of Systems, Control and Communications (IJSCC)*, no. Special Issue on Progress in Networked Control Systems, 2011, to Appear.

[4] C. A. Desoer and M. Vidyasagar, *Feedback Systems: Input-Output Properties*. Orlando, FL, USA: Academic Press, Inc., 1975.

[5] G. Niemeyer and J.-J. E. Slotine, "Telemanipulation with time delays," *International Journal of Robotics Research*, vol. 23, no. 9, pp. 873 – 890, 2004.

[6] R. Anderson and M. Spong, "Asymptotic stability for force reflecting teleoperators with time delay," *The International Journal of Robotics Research*, vol. 11, no. 2, pp. 135–149, 1992.

[7] N. Kottenstette and P. Antsaklis, "Relationships between positive real, passive dissipative, & positive systems," *American Control Conference*, pp. 409–416, 2010.

[8] G. Zames, "On the input-output stability of time-varying nonlinear feedback systems. i. conditions derived using concepts of loop gain, conicity and positivity," *IEEE Transactions on Automatic Control*, vol. AC-11, no. 2, pp. 228 – 238, 1966.

[9] J. C. Willems, *The Analysis of Feedback Systems*. Cambridge, MA, USA: MIT Press, 1971.

[10] N. Kottenstette and J. Porter, "Digital passive attitude and altitude control schemes for quadrotor aircraft," Dec. 2009, pp. 1761 –1768.

[11] N. Kottenstette and N. Chopra, "Lm2-stable digital-control networks for multiple continuous passive plants," *1st IFAC Workshop on Estimation and Control of Networked Systems (NecSys'09)*, 2009.

[12] S. Hirche and M. Buss, "Transparent Data Reduction in Networked Telepresence and Teleaction Systems. Part II: Time-Delayed Communication," *Presence: Teleoperators and Virtual Environments*, vol. 16, no. 5, pp. 532–542, 2007.

[13] N. Chopra, P. Berestesky, and M. Spong, "Bilateral teleoperation over unreliable communication networks," *IEEE Transactions on Control Systems Technology*, vol. 16, no. 2, pp. 304–313, 2008.

[14] S. Hirche, T. Matiakis, and M. Buss, "A distributed controller approach for delay-independent stability of networked control systems," *Automatica*, vol. 45, no. 8, pp. 1828–1836, 2009.

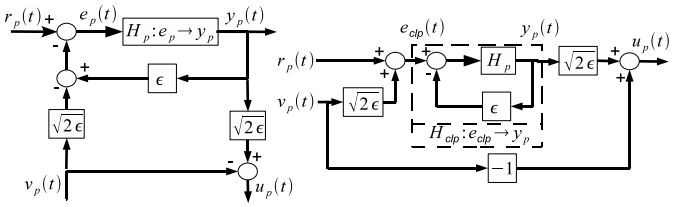

Fig. 9. Plant-r_p-v_p-y_p-u_p-network realization and initial transformation.

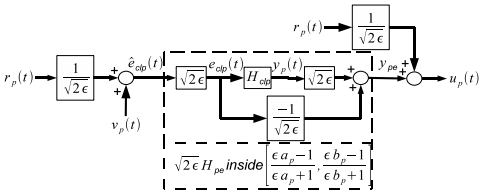

Fig. 10. Final Plant-r_p-v_p-y_p-u_p-network realization.

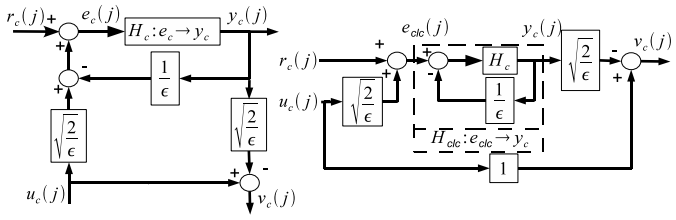

Fig. 11. Controller-r_c-u_c-e_p-v_c-network realization and initial transformation.

[15] M. Kuschel, P. Kremer, and M. Buss, "Passive haptic data-compression methods with perceptual coding for bilateral presence systems," *IEEE Transactions on Systems, Man and Cybernetics, Part A: Systems and Humans*, vol. 39, no. 6, pp. 1142 – 1151, Nov. 2009.

[16] D. J. Hill, "Dissipative nonlinear systems: Basic properties and stability analysis," *Proceedings of the 31st IEEE Conference on Decision and Control*, pp. 3259–3264, 1992.

[17] D. J. Hill and P. J. Moylan, "The stability of nonlinear dissipative systems," *IEEE Transactions on Automatic Control*, vol. AC-21, no. 5, pp. 708 – 11, 1976.

[18] ——, "Stability results for nonlinear feedback systems," *Automatica*, vol. 13, pp. 377–382, 1977.

[19] G. C. Goodwin and K. S. Sin, *Adaptive Filtering Prediction and Control*. Englewood Cliffs, New Jersey 07632: Prentice-Hall, Inc., 1984.

[20] W. M. Haddad and V. S. Chellaboina, *Nonlinear Dynamical Systems and Control: A Lyapunov-Based Approach*. Princeton, New Jersey, USA: Princeton University Press, 2008.

[21] N. Kottenstette, H. LeBlanc, E. Eyisi, and X. Koutsoukos, "Multi-rate networked control of conic systems," Institute for Software Integrated Systems, Vanderbilt University, Nashville, TN, Report, 2009. [Online]. Available: http://www.isis.vanderbilt.edu/node/4120

[22] R. J. Anderson and M. W. Spong, "Bilateral control of teleoperators with time delay," *Proceedings of the IEEE Conference on Decision and Control Including The Symposium on Adaptive Processes*, pp. 167 – 173, 1988.

[23] A. Oppenheim, A. Willsky, and S. Nawab, *Signals and systems*. Prentice hall Upper Saddle River, NJ, 1997.

[24] N. Kottenstette and P. Antsaklis, "Wireless Control of Passive Systems Subject to Actuator Constraints," *47th IEEE Conference on Decision and Control, 2008. CDC 2008*, pp. 2979–2984, 2008.

[25] S. Stramigioli, C. Secchi, A. J. van der Schaft, and C. Fantuzzi, "Sampled data systems passivity and discrete port-hamiltonian systems," *IEEE Transactions on Robotics*, vol. 21, no. 4, pp. 574 – 587, 2005.

[26] J.-H. Ryu, Y. S. Kim, and B. Hannaford, "Sampled- and continuous-time passivity and stability of virtual environments," *IEEE Transactions on Robotics*, vol. 20, no. 4, pp. 772 – 6, 2004.

[27] N. Kottenstette and P. Antsaklis, "Stable digital control networks for continuous passive plants subject to delays and data dropouts," *46th IEEE Conference on Decision and Control*, pp. 4433–4440, 2007.

[28] G. F. Franklin, J. D. Powell, and A. Emami-Naeini, *Feedback Control of Dynamic Systems*, 5th ed. Prentice-Hall, 2006.

APPENDIX I
WAVE VARIABLE NETWORK PROPERTIES

Fig. 9 depicts a graphical realization of (7) on the left-hand-side (LHS), and the first obvious graphical transformation on the right-hand-side (RHS) in which we denote closed-loop transformation of the plant H_p in terms of the feedback gain ϵ as $H_{\mathsf{clp}} : e_{\mathsf{clp}} \to y_p$ in which

$$e_{\mathsf{clp}}(t) = r_p(t) + \sqrt{2\epsilon} v_p(t) = e_p(t) + \epsilon y_p(t). \tag{20}$$

In order to simplify discussion and to leverage Theorem 1 we use Assumption 1 in order to derive Corollary 3:

Corollary 3: If Assumption 1 is satisfied then $H_{\mathsf{clp}} : e_{\mathsf{clp}} \to y_p$ is inside the sector $\left[\frac{a_p}{1+\epsilon a_p}, \frac{b_p}{1+\epsilon b_p}\right]$.

Next we transform the RHS realization in Fig. 9 to the final form depicted in Fig. 10.

Lemma 4: The RHS of Fig. 9 can be transformed to the final form depicted in Fig. 10 (in which $H_{\mathsf{pe}} e_{\mathsf{clp}} = \sqrt{2\epsilon} H_{\mathsf{clp}} e_{\mathsf{clp}} - \frac{1}{\sqrt{2\epsilon}} e_{\mathsf{clp}}$). In addition if Assumption 1 is satisfied, then $\sqrt{2\epsilon} H_{\mathsf{pe}} \hat{e}_{\mathsf{clp}}(t)$ is inside the sector $\left[\frac{\epsilon a_p - 1}{\epsilon a_p + 1}, \frac{\epsilon b_p - 1}{\epsilon b_p + 1}\right]$. See proof in [21]. Fig. 11 depicts a graphical realization of (8) on the left-hand-side (LHS), and the first obvious graphical transformation on the right-hand-side (RHS) in which we denote closed-loop transformation of the controller H_c in terms of the feedback gain $\frac{1}{\epsilon}$ as $H_{\mathsf{clc}} : e_{\mathsf{clc}} \to y_c$ in which

$$e_{\mathsf{clc}}(j) = r_c(j) + \sqrt{\frac{2}{\epsilon}} u_c(j) = e_c(j) + \frac{1}{\epsilon} y_c(j). \tag{21}$$

Which allows us to state the following corollary:

Corollary 4: If Assumption 1 is satisfied then $H_{\mathsf{clc}} : e_{\mathsf{clc}} \to y_c$ is inside the sector $\left[\frac{\epsilon a_c}{\epsilon + a_c}, \frac{\epsilon b_c}{\epsilon + b_c}\right]$.

Next we transform the RHS realization in Fig. 11 to the final form depicted in Fig. 12.

Lemma 5: The RHS of Fig. 11 can be transformed to the final form depicted in Fig. 12 (in which $H_{\mathsf{ce}} e_{\mathsf{clc}} = -\sqrt{\frac{2}{\epsilon}} H_{\mathsf{clc}} e_{\mathsf{clc}} + \sqrt{\frac{\epsilon}{2}} e_{\mathsf{clc}}$). In addition if Assumption 1 is satisfied, then $\sqrt{\frac{2}{\epsilon}} H_{\mathsf{ce}} \hat{e}_{\mathsf{clc}}(j)$ is inside the sector $\left[\frac{\epsilon - b_c}{\epsilon + b_c}, \frac{\epsilon - a_c}{\epsilon + a_c}\right]$. See proof in [21].

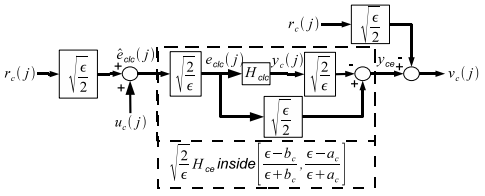

Fig. 12. Final Controller-r_c-u_c-y_c-v_c-network realization.